High Temperature Fiber Bragg Gratings for Spacecraft Application

Richard J. Black and Behzad Moslehi
Intelligent Fiber Optic Systems Corporation (IFOS)
rjb@ifos.com; bm@ifos.com

Abstract: Spacecraft require sensors operating over extreme temperature ranges. Silica Fiber Bragg grating sensors can have application from cryogenic temperatures to between 1000 and 1200 °C dependent on operation time. Thermal protection systems provide application examples.
OCIS codes: (060.2370) Fiber optics sensors; (060.3738) Fiber Bragg Gratings;

1. Introduction

The space environment provides an extreme range of temperatures. Fiber Bragg grating (FBG) sensors can have spacecraft application from cryogenic temperatures to over 1200 °C with example applications being fuel tanks, such as Compressed Overwrapped Pressure Vessels (COPVs), and thermal protection systems (TPS) [1-7]. For small probes undergoing a single atmospheric entry during their lifetime, high-temperature survivability over minutes may be sufficient. This contrasts with reusable spacecraft and terrestrial applications such as turbine engines for power plants [8] and aircraft [9, 10] where survivability and accurate measurement may be required for tens of thousands of hours.

2. High Temperature FBG Measurements

Regenerated gratings [11-15] have been considered for ultra-high temperature applications. These require appropriate handling and packaging because of the brittleness resulting from the annealing process. On the other hand, integration into a structure, such as a TPS is easier if the fiber still has its jacket to provide added mechanical stability, which usually means that it should happen before any annealing (unless that annealing can be done during the draw-tower process before jacketing the fiber). Write-through-the jacket, femtosecond laser written FBGs have shown good temperature stability to 1025 °C [8]. They may be used to even higher temperatures for applications, requiring only short exposure, as may occur in single entry aero-capture, such as measured by thermocouples in the "seven-minutes-of-terror" Mars Science Laboratory results of [2]. Longer term exposure, however, can result in a permanent wavelength offset (as will be seen in Fig. 4).

Single Monotonic Heating to 1200 °C in Minutes and Cooling: In Fig. 1(a) we show an example result of an infrared femtosecond laser written FBG in silica "pure-core" fiber (fluorine doped inner cladding) heated to 1200 °C in a tube oven. In the heating part of the measurement, the FBG responded faster to temperature change than the Type K thermocouple probe. Thus the much slower cool-down is typically used for calibration as in [5] and below.

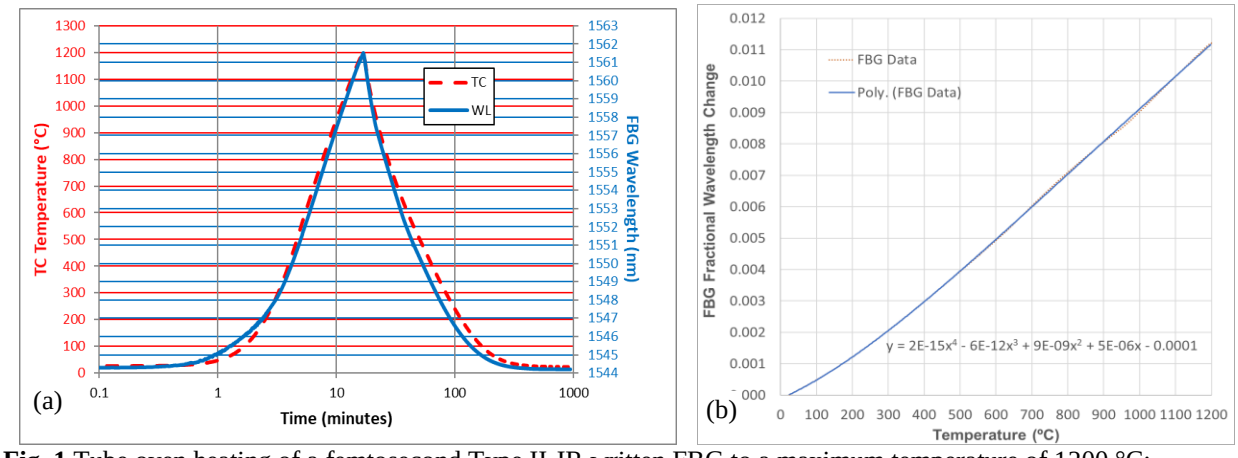

Fig. 1 Tube oven heating of a femtosecond Type II-IR written FBG to a maximum temperature of 1200 °C: (a) thermocouple temperature and FBG wavelength vs. time, (b) calibration curve from cool-down.

Calibration Curves: Fig. 1(b) shows the fractional wavelength change $\delta\lambda/\lambda$ (with respect to the room-

temperature wavelength) vs. temperature T. The inverse result (T vs. $\delta\lambda/\lambda$) is, in this case,

$$T\,/\,°C = -5.549\text{x}10^{10}(\delta\lambda/\lambda)^4 + 1.501\text{ x }10^{9}(\delta\lambda/\lambda)^3 - 1.479\text{x}10^{7}(\delta\lambda/\lambda)^2 + 158991(\delta\lambda/\lambda) + 24.0 \quad (1)$$

This is close to the cubic polynomial dependence obtained in [5] up to 1000 °C for a femtosecond laser written FBG in standard germanium doped core silica fiber. As seen in Fig. 2, above 1000 °C, the quartic term enables a better fit over the complete temperature range for short term exposure (minutes). Alternatively, a piecewise fit may be used. In particular, while the nonlinear dependence is particularly apparent below 300 °C (and increases towards absolute zero - [5] and the piecewise fit of Sec. 4 - Fig. 7), above 300 °C, it is reasonably linear with a fractional wavelength increase of 0.0010 corresponding to a 100 °C temperature increase (i.e., 15.5 pm/°C at 1550 nm up from the well-known room temperature rule-of-thumb result 10-11pm/°C at 1550 nm). Above 1000 °C, the fractional wavelength increase is slightly greater (tending to 0.0011 per 100°C, corresponding to 17 pm/°C at 1550 nm).

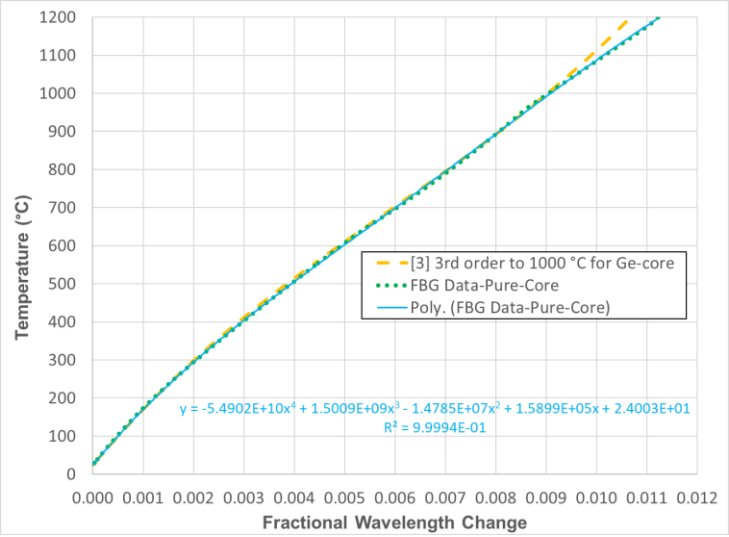

Fig. 2 Temperature versus fractional wavelength change calibration curve to 1200 °C deduced from Fig. 1 measurements in comparison with the 1000 °C calibration curve given as Eq. 4 of [5].

Temperature Cycling: In the following graphs, we show results for temperature cycling in a laboratory tube oven filled with inert (argon) gas of FBGs written with femtosecond pulses at 800 nm.

Multiple Cycles up to 1000 °C: In the first test, which involved cycling up to 800 °C for nearly 3 hours, then up to 1000 °C for 15 hours (to hour 18) and then cooling, as shown in Fig. 3, the initial wavelength 1538.7 nm was maintained at the end of the 26-hour test (as was the FBG intensity).

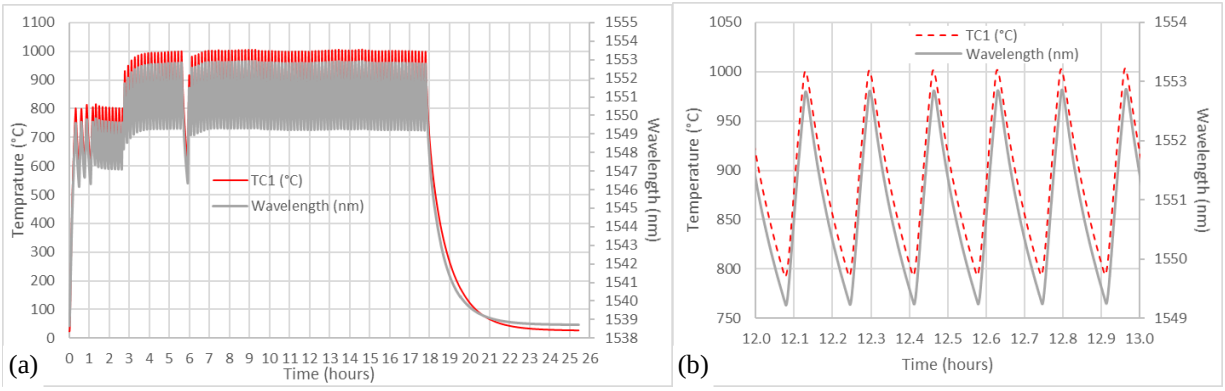

Fig. 3 Temperature cycling of a femtosecond Type II-IR written FBG to a maximum temperature of 1000 °C.

Multiple Cycles above 1000 °C: By contrast, cycling to temperatures over 1000 °C (to 1150 °C) as in the Fig. 4 example, led to a gradual permanent increase of the Bragg wavelength Fig. 4(a,b) as well as a decrease in the

strength of the FBG - Fig. 4(c). Nevertheless, for short-term applications, some useful information about temperature can be deduced.

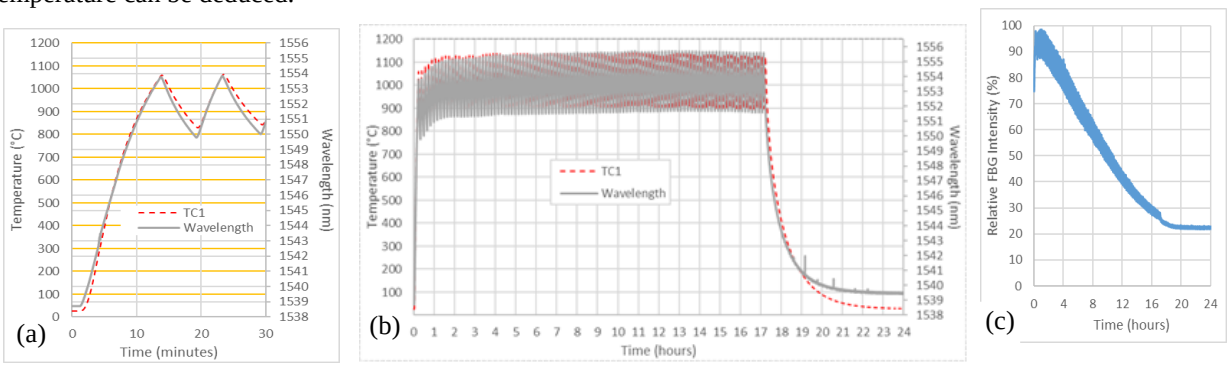

Fig. 4 Temperature cycling of a Type II-IR written FBG to a maximum temperature of 1150 °C.

3. Reusable and Ablative Thermal Protection System (TPS) Sensor Examples

Spacecraft rely on TPS to provide shielding of the vehicle structure and payload from the high heating encountered during launch and atmospheric aero-capture or entry/reentry. Reliable TPS sensors can provide data useful in optimizing spacecraft heat shield designs using both ablative and reusable TPS technologies.

(a) Reusable TPS Example: Fig. 5 shows an example setup for temperature monitoring with 2 FBG arrays (one horizontal and the other diagonal) in the bondline between two reusable thermal TPS tiles subjected to heat from one side, as may be the case for a re-entry vehicle. Fig. 5(a) shows that as one side of the tile was exposed to up to 540 °C, all FBG sensors survived and tracked temperature at different depths through the TPS tile cross-section. Fig. 5(b) shows the temperature profile for the horizontal array on the cold side of the TPS, and Fig. 5(c) gives a 1-D approximation to the heat flux determined from the temperature differences between FBG pairs on the two arrays.

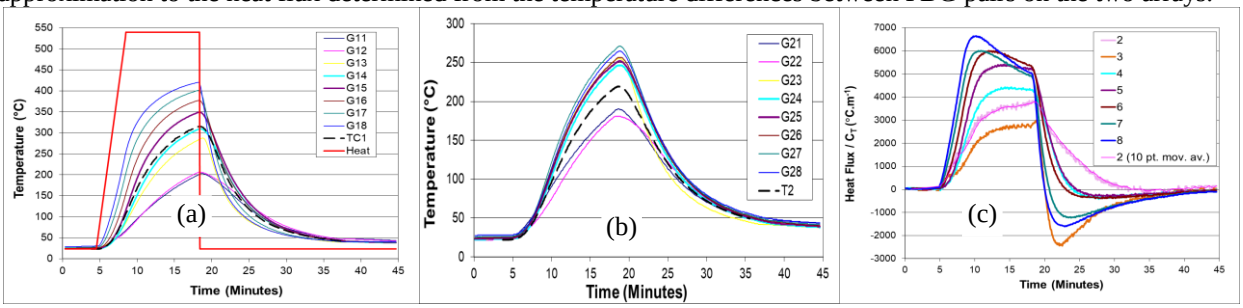

Fig. 5 Reusable TPS coupon: (a) Temperature evolution at different depths in TPS measured with a diagonally oriented 8-FBG array [16]. (b) Temperature evolution for a horizontal 8-FBG near the cold side of the TPS with horizontal positions matching those of the diagonal array. (d) Heat flux normalized with respect to thermal conductivity for the separated pairs of FBGs.

(b) Ablative TPS Example: In Fig. 6, we present results [3] for arc jet testing of an ablative TPS coupon, undergoing conditions representative of simulated atmospheric entry [1]. The FBGs provide good temperature data to 1000 °C, and some useful information above that temperature for a limited time period.

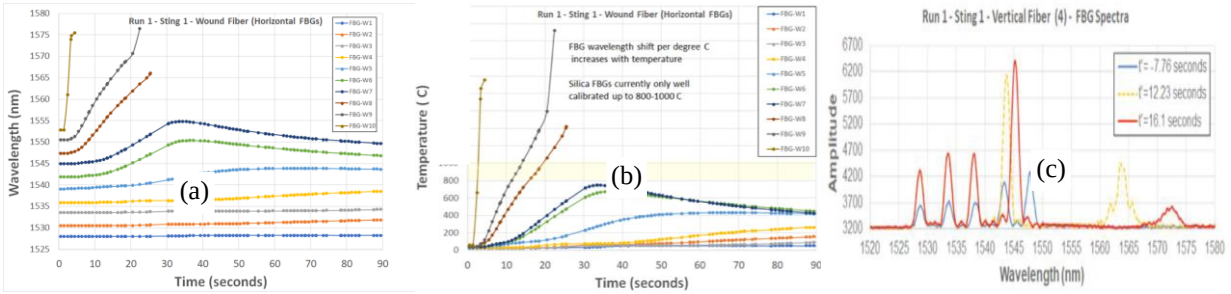

Fig. 6 Ablative TPS coupon with 25 second arc jet exposure: (a, b) 10 FBG sensors oriented perpendicular to heat flux: (b) wavelength vs. time, (c) temperature vs. time, (d) spectra for 5 FBG sensors parallel to heat flux direction.

4. Discussion and Extension to Cryogenic Temperatures

Femtosecond laser written FBGs are promising candidates for high temperature measurements. While annealing is known to increase long-term temperature stability (through stress relaxation, for example), structural integration is often easier prior to annealing when the fiber still possesses a buffer jacket, e.g., polyimide, and annealing-induced embrittlement has not yet occurred. As such, femtosecond laser written FBGs in pure-core fiber can still provide some useful short-term results even up to 1200°C. If longer-term high-temperature usage is required, then the permanent wavelength shifts resulting from annealing must be taken into account. The FBG sensors can also be used for cryogenic measurements [17, 18]. In this case, however, the wavelength-change per degree Celsius is significantly reduced with the respect to the high temperature result according to the cubic polynomial expression given in [5] and the piecewise fit in Fig. 7. Thus temperature measurement is better achieved through integration of the fiber with a material with a larger low-temperature thermal expansion coefficient [19].

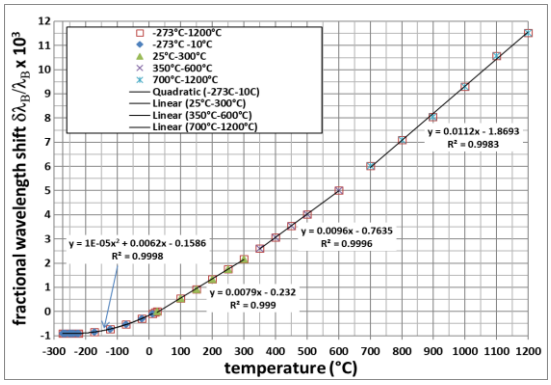

Fig. 7 Piecewise fit to example fractional wavelength versus temperature data from -270 to 1200 °C.

5. References

[1] R. A. Beck, D. M. Driver, M. J. Wright, H. H. Hwang, K. T. Edquist, and S. A. Sepka, "Development of the Mars Science Laboratory heatshield thermal protection system," *Journal of Spacecraft and Rockets*, vol. 51, no. 4, pp. 1139-1150, 2014.

[2] A. Little, D. Bose, C. Karlgaard, M. Munk, C. Kuhl, M. Schoenenberger, C. Antill, R. Verhappen, P. Kutty, and T. White, "The Mars Science Laboratory (MSL) Entry, Descent and Landing Instrumentation (MEDLI): Hardware Performance and Data Reconstruction," presented at the AAS, 2013.

[3] R. J. Black, J. D. Feldman, D. Ellerby, J. Monk, B. Moslehi, L. Oblea, and M. Switzer, "Fiber Optic Temperature Sensors in TPS: Arc Jet Model Design & Testing - 2nd prize poster," presented at the NSMMS/CASTE 2017, Indian Wells, CA, 2017.

[4] R. J. Black, J. M. Costa, B. Moslehi, L. Zarnescu, D. Hackney, and K. Peters, "Fiber optic temperature profiling for thermal protection heat shields," in *Smart Sensor Phenomena, Technology, Networks, and Systems Integration 2014, Proc. SPIE 9062*, San Diego, 2014, vol. Proc. SPIE 9062, pp. 906204-1 to 906204-12: SPIE, 2014.

[5] R. J. Black, J. M. Costa, L. Zarnescu, D. A. Hackney, B. Moslehi, and K. J. Peters, "Fiber-optic temperature profiling for thermal protection system heat shields," *Optical Engineering*, vol. 55, no. 11, pp. 114101-114101, 2016.

[6] R. J. Black, K. Chau, L. K. Good, M. Hernandez, L. Oblea, and B. Moslehi, "Fiber-Optic Sensing for Thermal Protection Structures in Vehicle Health Monitoring," presented at the Proc. Quantitative Non Destructive Evaluation (QNDE), 2005.

[7] R. J. Black, K. Chau, L. K. Good, and B. Moslehi, "High-temperature fiber optic sensors for integrated systems health management," *Proc. 17th Aeromat Conference & Exhibition (invited paper)*, 2006.

[8] R. B. Walker, S. J. Mihailov, D. Grobnic, C. Hnatovsky, P. Lu, H. Ding, D. Coulas, and M. De Silva, "Femtosecond Laser Written Fiber Bragg Grating Sensors for Combustion Environments," in *Bragg Gratings, Photosensitivity and Poling in Glass Waveguides and Materials*, 2018, p. BM4A. 1: Optical Society of America.

[9] J. M. Costa, R. J. Black, B. Moslehi, and A. R. Behbahani, "Advances in high temperature fiber optic sensors for turbine engine applications," in *58th International Instrumentation Symposium (IIS)*, San Diego, 2012: International Society of Automation (ISA), 2012.

[10] G. Adamovsky, J. R. Mackey, L. A. Kren, B. M. Floyd, K. A. Elam, and M. Martinez, "Development and Performance Verification of Fiber Optic Temperature Sensors in High Temperature Engine Environments," in *50th AIAA/ASME/SAE/ASEE Joint Propulsion Conference: Propulsion and Energy Forum* Cleveland, OH 2014, vol. AIAA 2014-3922 pp. 1-12: AIAA.

[11] J. Canning, "Regenerated gratings for optical sensing in harsh environments," *Bragg Gratings, Photosensitivity, and Poling in Glass Waveguides*, p. BTu3E. 3, OSA, 2012.

[12] G. Adamovsky, S. F. Lyuksyutov, J. R. Mackey, B. M. Floyd, U. Abeywickrema, I. Fedin, and M. Rackaitis, "Peculiarities of thermo-optic coefficient under different temperature regimes in optical fibers containing fiber Bragg gratings," *Optics Communications*, vol. 285, no. 5, pp. 766-773, 2012.

[13] G. Laffont, R. Cotillard, N. Roussel, R. Desmarchelier, and S. Rougeault, "Temperature Resistant Fiber Bragg Gratings for On-Line and Structural Health Monitoring of the Next-Generation of Nuclear Reactors," *Sensors (Basel, Switzerland)*, vol. 18, no. 6, 2018.

[14] M. Lindner, E. Tunc, K. Weraneck, F. Heilmeier, W. Volk, M. Jakobi, A. W. Koch, and J. Roths, "Regenerated Bragg Grating Sensor Array for Temperature Measurements During an Aluminum Casting Process," *IEEE Sensors Journal*, vol. 18, no. 13, pp. 5352-5360, 2018.

[15] M. Lancry, K. Cook, D. Pallarés-Aldeiturriaga, J. Lopez-Higuera, B. Poumellec, and J. Canning, "Raman spectroscopic study of Bragg gratings regeneration," in *Bragg Gratings, Photosensitivity and Poling in Glass Waveguides and Materials*, OSA, 2018, p. BM2A. 4.

[16] R. J. Black and B. Moslehi, "Advanced end-to-end fiber optic sensing systems for demanding environments," in *SPIE Optical Engineering+ Applications*, 2010, vol. Proc. SPIE 7817, pp. 78170L-78170L-9: International Society for Optics and Photonics, 2010.

[17] J. Roths, G. Andrejevic, R. Kuttler, and M. Süßer, "Calibration of fiber Bragg cryogenic temperature sensors," in *Optical Fiber Sensors*, 2006, p. TuE81: Optical Society of America.

[18] U. Sampath, D. Kim, H. Kim, and M. Song, "Polymer-coated FBG sensor for simultaneous temperature and strain monitoring in composite materials under cryogenic conditions," *Applied Optics*, vol. 57, no. 3, pp. 492-497, 2018.

[19] C. Vendittozzi, F. Felli, and C. Lupi, "Modeling FBG sensors sensitivity from cryogenic temperatures to room temperature as a function of metal coating thickness," *Optical Fiber Technology*, vol. 42, pp. 84-91, 2018.